

# Design, fabrication, and impedance of plasma wave detectors

Sungmu Kang<sup>a</sup>, Peter J. Burke<sup>a</sup>, L. N. Pfeiffer<sup>b</sup>, K. W. West<sup>b</sup>

<sup>a</sup>Henry Samueli School of Engineering, Electrical Engineering and Computer Science,  
Intergrated Nanosystems Research Facility

University of California, Irvine, CA, USA 92697-2625;

<sup>b</sup>Bell Laboratories, Lucent Technologies, Murray Hill, NJ, USA 07974

## Abstract

We present the design, fabrication, and impedance measurements of plasma wave detectors fabricated from GaAs/AlGaAs heterostructures. The design principles will allow broadband (dc to 7 GHz) measurements of the device power coupling and responsivity as a detector, which is a “scale model” of a THz plasma wave detector. We demonstrate clear resonance behavior in the impedance spectrum.

Keywords: HEMT, THz, plasma wave electronics

## 1. INTRODUCTION

As the gate length of modern devices becomes comparable to the mean free path, electrons can move without scattering (ballistic transport) from source to drain. In a related phenomenon, when the frequency is larger than the scattering frequency, the transport is also ballistic in the sense that electrons move without scattering between electric field cycles. At room temperature, the scattering frequency is about 500 GHz, while at cryogenic temperatures, the frequency can be around 1 GHz because of the reduced phonon scattering. How does a high electron mobility transistor (HEMT) behave in this ballistic ( $\omega\tau > 1$ ) regime? The answer to this question is the realm of plasma wave electronics[1-12]. Such a broad class of devices could have many applications in military, medical, and biological applications such as remote standoff chemical and biological detection and species identification.

Shur has a theory for the use of a HEMT in the ballistic limit as a detector of THz radiation[1-12]. In the proposed device, three conditions must be satisfied: 1) An ac voltage is applied to the gate, 2) The source is grounded at both ac and dc, and 3) The drain is an open circuit at ac, i.e. no ac current flows through the drain. Under these conditions, at resonant frequencies given by  $f = n v_p / 4 L_{\text{gate}}$  (with  $v_p$  the plasma wave velocity), a dc voltage develops at the drain, hence the device performs as a detector. In order to readout this dc voltage, the drain must be contacted at dc. Such a device is named a plasma wave detector. In this paper we discuss the design, fabrication, and impedance of a device that realize these conditions.

To date, responsivity measurements have been performed at fixed frequencies in the THz range of such devices[1-12]. These initial measurements are significant and important. However these initial experiments did not allow for swept frequency broadband measurements, and did not quantitatively determine the power coupling from the ac generator to the device. It is the purpose of this work to design experiments that allow swept-frequency measurements and quantitative power coupling measurements in order to quantitatively determine the intrinsic device performance over a broad range of frequencies. In order to do this, we perform measurements on long HEMTs at cryogenic temperatures so that the resonant frequencies are in the microwave (dc-10 GHz) frequency range.

It is the purpose of this paper to describe the design, fabrication, and initial impedance matching measurements of such a plasma wave detector. We achieve a broadband ac open circuit at the drain by using a long, highly resistive thin strip of NiCr on chip, which allows us to make dc contact to the drain in order to measure the responsivity while at the same time preventing ac current from flowing into the drain. In addition, we measure the gate-source impedance vs. frequency in order to determine the power coupling to our 50  $\Omega$  system. This will allow future quantitative tests of Shur’s theory of plasma wave detectors.

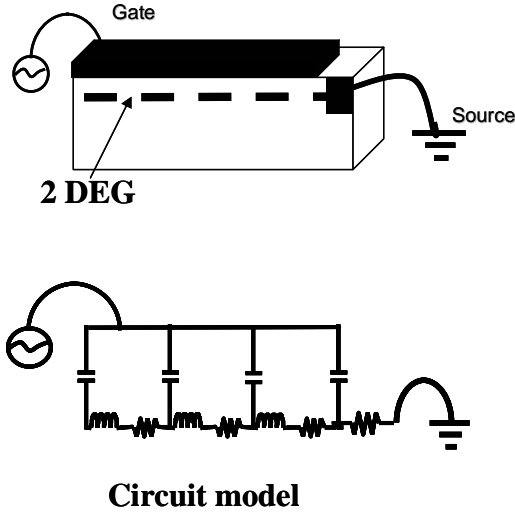


**Fig. 1:** Diagram and ac circuit model for a plasma wave detector. The drain is contacted at dc (not shown).

## 2. THEORY AND BACKGROUND

In this paper, we consider the ac equivalent circuit of the geometry shown in Fig. 1. In this case, an ac voltage is applied to the gate while the source is grounded. (No ac current flows through the drain). We recently showed[13, 14] that from diffusive ( $\omega\tau < 1$ ) to ballistic transport ( $\omega\tau > 1$ ), the ohmic contact impedance of a two dimensional electron gas is real and independent of the frequency in the microwave range if the mobility is higher than  $500,000 \text{ cm}^2/\text{V}\cdot\text{s}$ . If the source contact resistance ( $R_{\text{source-contact}}$ ) is ohmic, the impedance of the gated two dimensional electron gas[15] can be written as

$$Z_{\text{gate-source}} = R_{\text{source-contact}} + \sqrt{\frac{R_{2\text{DEG}} + i\omega L_k}{i\omega C}} \coth\left(L_{\text{gate}} \sqrt{(R_{2\text{DEG}} + i\omega L_k) i\omega C}\right). \quad (1)$$

This impedance determines how much power is absorbed by the device and hence its responsivity as a detector.

At high frequency, Real ( $Z_{\text{gate-source}}$ ) shows resonance peaks at the fundamental frequency ( $f_{\text{peak}} = v_p / 2L_{\text{gate}}$ ) and its harmonics. In this model, the plasma wave velocity is given by:

$$v_p = f_{\text{peak}} 2L_{\text{gate}} = \sqrt{\frac{ne^2 d}{m^* \epsilon}}, \quad (2)$$

where  $n$  is the density,  $d$  the depth down, and  $\epsilon$  the dielectric constant.

**Table 1.** Summary of measured values from wafer (nominal) and devices.

Sample	Electron density (/cm <sup>2</sup> )	Nominal Mobility (cm <sup>2</sup> /Vs)	R <sub>2DEG</sub> (Ω)	R <sub>sd</sub> (Ω)	R <sub>contact</sub> (Ω)	τ <sub>nominal</sub> ≡ μm <sup>2</sup> /e (ps)
1	1.13 10 <sup>11</sup>	3.26 10 <sup>6</sup>	68	120 (±15)	52 (±15)	120
2	2.06 10 <sup>11</sup>	6.00 10 <sup>6</sup>	22	70 (±20)	48 (±20)	230

### 3. FABRICATION

The plasma wave detector is fabricated from GaAs/AlGaAs modulation doped single quantum well heterostructure grown by molecular beam epitaxy. The gate length ( $L_{\text{gate}}$ ) is 200 μm and the width is 50 μm. The depth of the 2DEG is 1900 Å. Two samples with the same geometry but different electron density and mobility were prepared. Table 1 shows the nominal mobility and electron density based on dc measurements. Because of the large dc series resistance of the NiCr, dc measurements of the source-drain resistance and contact resistance are approximate.

After MBE growth, a mesa is defined with wet etching. The mesa size is 50μm × 200μm and the depth of the mesa is ~8000Å. Ni/Ge/Au/Ni/Au ohmic metallization (80:270:540:140:2000Å) is carried out by electron beam evaporation. Rapid thermal annealing follows after metallization for 12 min. at 440°C. Ti/Au (300:3000Å) metallization is used to form the gate. The narrow strip (20μm × 1500μm) of NiCr (80-20 wt %) (200Å /800Å) is deposited from the drain in order to have pure resistance (~ 1 kΩ) with little capacitance to ground. Before the measurement, a red light is illuminated on sample 2 for 2 min in order to achieve the necessary electron density and mobility; sample 1 is used without light illumination. A device image is shown in Fig. 2.

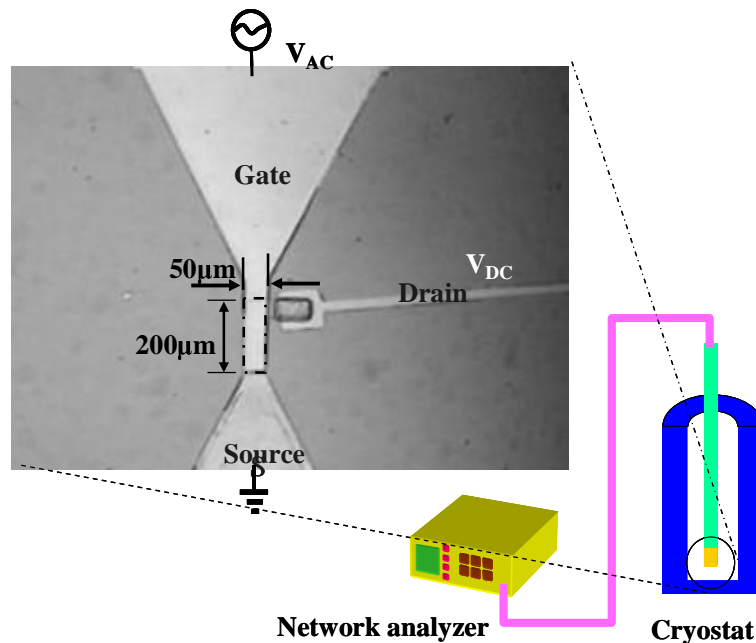


**Fig. 2:** Measurement setup for impedance.

#### 4. MEASUREMENTS

In order to characterize the plasma wave detector, we measure the impedance of two devices with different mobility and electron density. The dc impedance is measured with a lock-in amplifier. We measure total resistance of source to drain ( $R_{sd}=R_{contact} + R_{2DEG}$ ) and the NiCr film in series. The NiCr film resistance is estimated from dc sheet resistance measurements at 4 K. All measurements were performed at 4 K.

For the ac measurement, the sample is mounted at the end of 50  $\Omega$  matched microstrip line and soldered with indium into place. The reflection coefficient ( $S_{11}=V_{reflected}/V_{incident}$ ) of the sample is measured by a network analyzer (Agilent 8270 ES) from 50 MHz to 7 GHz at 100 nW. The impedance is characterized by inverting the reflection coefficient ( $S_{11}=[Z(\omega)-50]/[Z(\omega)+50]$ ). The detailed calibration technique was presented in a previous report[13]. A gate bias can be applied through a bias tee during the measurement. Figs. 1 and 2 show the impedance and measurement setup respectively.

#### 5. RESULTS AND DISCUSSION

Fig.3 shows the real impedance of sample 1 as a function of frequency.  $Re(Z(\omega))$  shows clear plasma wave resonances. The measured resonance peaks ( $f_{peak}$ ) occur at around 2.2 and 4.5 GHz respectively, which satisfy the expectation from equation 2. The measured  $Re(Z(\omega))$  agrees with the theoretical expectation of equation 1 when the source contact resistance ( $R_{source\_contact}$ ) is 27  $\Omega$ .

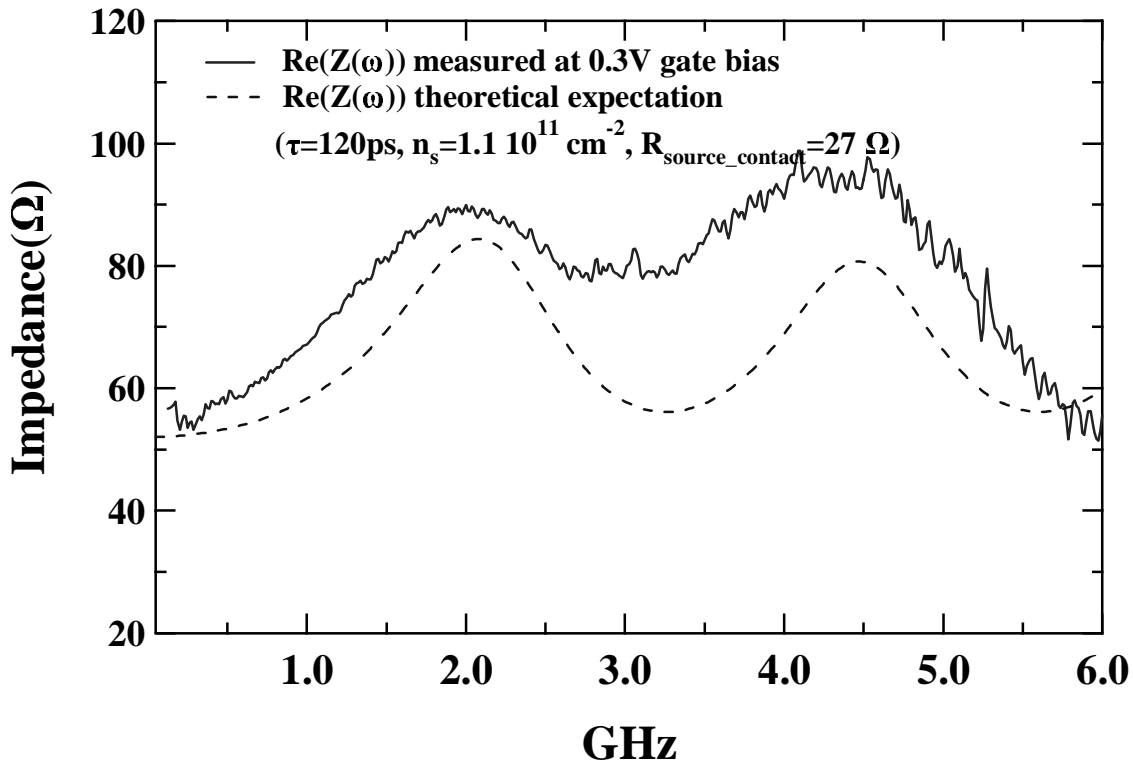


**Fig. 3:** Impedance of plasma wave detector with nominal mobility ( $3.26 \cdot 10^6 \text{ cm}^2/\text{V}\cdot\text{s}$ ).

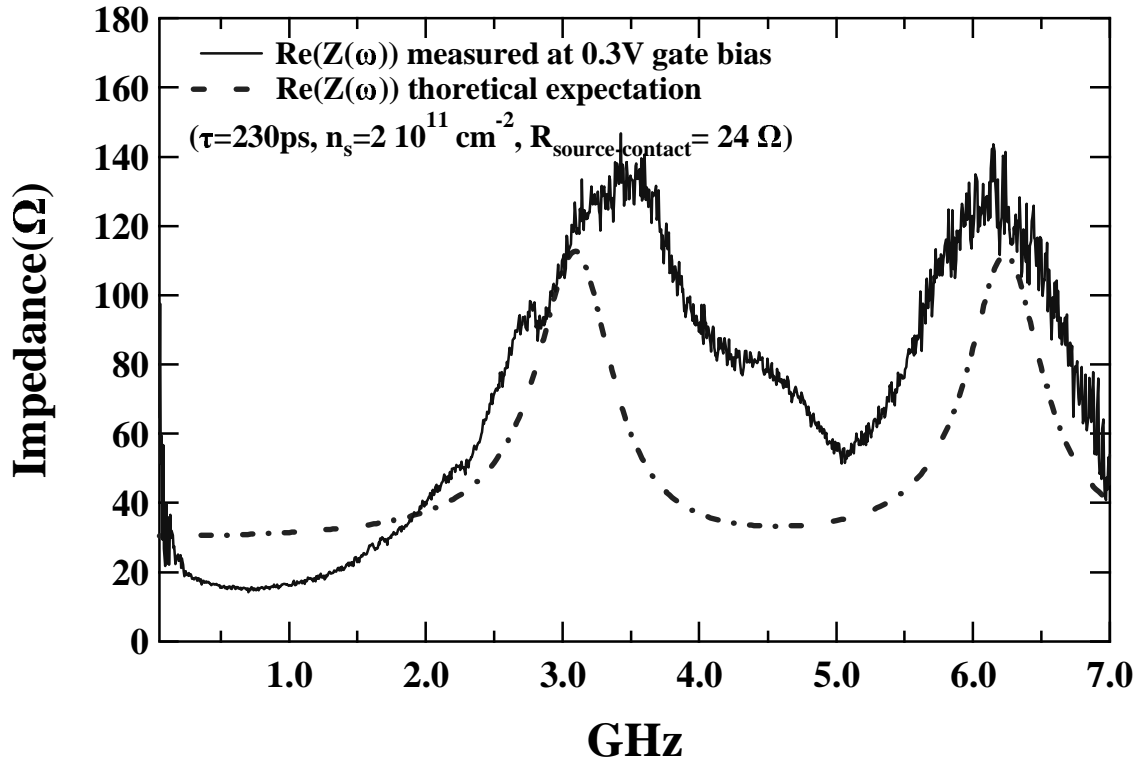


**Fig. 4:** Impedance of plasma wave detector with mobility ( $6.00 \cdot 10^6 \text{ cm}^2/\text{V}\cdot\text{s}$ ).

Fig.4 shows the measured  $\text{Re}(Z(\omega))$  of sample 2 and the theoretical expectation.  $\text{Re}(Z(\omega))$  shows resonance peaks at 3.2 GHz and 6 GHz, which agrees with equation 2. When we use  $R_{\text{source-contact}}$  as  $24 \Omega$ , the measured values and theoretical expectation agree with each other over the entire frequency range. The results from both samples are summarized in Table 2. In all cases, we have quantitatively determined the power coupling to the device over a broad range of frequencies.

**Table 2.** Summary of measured values with same geometry ( $50\mu\text{m}\times 200\mu\text{m}$ )

Sample	Electron density ( $/\text{cm}^2$ )	Nominal Mobility ( $\text{cm}^2/\text{Vs}$ )	$f_{\text{feak}}$ (GHz)	$V_p$ (m/s)	$R_{\text{source-contact}}$ ( $\Omega$ )	$L_k$ ( $\mu\text{H}/\text{m}$ )	C (nF/m)
1	$1.13 \cdot 10^{11}$	$3.26 \cdot 10^6$	2.2	$0.9 \cdot 10^6$	$27 (\pm 7)$	40	28
2	$2.06 \cdot 10^{11}$	$6.00 \cdot 10^6$	3	$1.2 \cdot 10^6$	$24 (\pm 10)$	23	28

## 6. CONCLUSIONS

We have presented the design, fabrication, and impedance matching measurements of a plasma wave detector. Future measurements will allow quantitative, broadband, frequency dependent responsivity measurements to be performed in order to ascertain intrinsic device performance as a plasma wave detector.

## ACKNOWLEDGMENTS

This work is supported by the National Science Foundation, Office of Naval Research, and the Army Research Office.

## REFERENCES

1. M. Dyakonov and M. Shur, "Detection, Mixing, and Frequency Multiplication of Terahertz Radiation by Two-Dimensional Electronic Fluid", *IEEE Transactions on electron devices*, 43, 380, (1996).
2. M. S. Shur and J. Q. Lu, "Terahertz Sources and Detectors Using Two-Dimensional Electronic Fluid in High Electron-Mobility Transistors", *IEEE Transactions on Microwave Theory and Techniques*, 48, 750-756, (2000).
3. J. Q. Lu and M. S. Shur, "Terahertz Detection by High-Electron-Mobility Transistor: Enhancement by Drain Bias", *Applied Physics Letters*, 78, 2587-2588, (2001).
4. M. S. Kushwaha and P. Vasilopoulos, "Resonant Response of a Fet to an Ac Signal: Influence of Magnetic Field, Device Length, and Temperature", *IEEE Transactions on Electron Devices*, 51, 803-813, (2004).
5. F. Teppe, Y. M. Meziani, N. Dyakonova, J. Lusakowski, F. Bauf, T. Skotnicki, D. Maude, S. Rumyantsev, M. S. Shur and W. Knap, "Terahertz Detectors Based on Plasma Oscillations in Nanometric Silicon Field Effect Transistors", *Physica Status Solidi(c)*, 2, 1413-1417, (2005).
6. W. Knap, F. Teppe, Y. Meziani, N. Dyakonova, J. Lusakowski, F. Boeuf, T. Skotnicki, D. Maude, S. Rumyantsev and M. S. Shur, "Plasma Wave Detection of Sub-Terahertz and Terahertz Radiation by Silicon Field-Effect Transistors", *Applied Physics Letters*, 85, 675-677, (2004).
7. A. V. Antonov, V. I. Gavrilenko, E. V. Demidov, S. V. Morozov, A. A. Dubinov, J. Lusakowski, W. Knap, N. Dyakonova, E. Kaminska, A. Piotrowska, K. Golaszewska and M. S. Shur, "Electron Transport and Terahertz Radiation Detection in Submicrometer-Sized Gaas/Algaas Field-Effect Transistors with Two-Dimensional Electron Gas", *Physics of the Solid State*, 46, 146-149, (2004).
8. J. Lusakowski, W. Knap, N. Dyakonova, L. Varani, J. Mateos, T. Gonzalez, Y. Roelens, S. Bollaert, A. Cappy and K. Karpierz, "Voltage Tuneable Terahertz Emission from a Ballistic Nanometer Ingaas/Inalas Transistor", *Journal of Applied Physics*, 97, -, (2005).
9. J. Lusakowski, F. Teppe, N. Dyakonova, Y. M. Meziani, W. Knap, T. Parenty, S. Bollaert, A. Cappy, V. Popov and M. S. Shur, "Terahertz Generation by Plasma Waves in Nanometer Gate High Electron Mobility Transistors", *Physica Status Solidi a-Applications and Materials Science*, 202, 656-659, (2005).
10. W. Knap, Y. Deng, S. Rumyantsev, J. Q. Lu, M. S. Shur, C. A. Saylor and L. C. Brunel, "Resonant Detection of Subterahertz Radiation by Plasma Waves in a Submicron Field-Effect Transistor", *Applied Physics Letters*, 80, 3433-3435, (2002).
11. W. Knap, Y. Deng, S. Rumyantsev and M. S. Shur, "Resonant Detection of Subterahertz and Terahertz Radiation by Plasma Waves in Submicron Field-Effect Transistors", *Applied Physics Letters*, 81, 4637-4639, (2002).
12. W. Knap, J. Lusakowski, T. Parenty, S. Bollaert, A. Cappy, V. V. Popov and M. S. Shur, "Terahertz Emission. By Plasma Waves in 60 Nm Gate High Electron Mobility Transistors", *Applied Physics Letters*, 84, 2331-2333, (2004).
13. S. Kang, P. J. Burke, L. N. Pfeiffer and K.W.West, "Ballistic Transport at Ghz Frequencies in Ungated Hemt Structures", *Solid State Electronics*, 48, 2013-2017, (2004).
14. S. Kang, P. J. Burke, L. N. Pfeiffer and K.W.West, "Ac Ballistic Transport in a Two Dimensional Electron Gas", *Physical Review B*, In Press, (2005).
15. P. J. Burke, I. B. Spielman, J. P. Eisenstein, L. N. Pfeiffer and K. W. West, "High Frequency Conductivity of the High-Mobility Two-Dimensional Electron Gas", *Applied Physics Letters*, 76, 745-747, (2000).